Radiation of USB-WLAN antenna influenced by human tissue and by notebook enclosure

W. Renhart, K. Hollaus, C. Magele, G. Matzenauer, *IEEE Student Member* and B. Weiss

***Abstract*— A standard WLAN-antenna operating at 2.4 GHz, connected to a PC-notebook has been investigated. In practise, both the presence of human biological tissue and of the notebook casing influence the antenna radiation pattern significantly. For determining the distortion, several numerical investigations have been accomplished. Thereby, variant configurations have been computed and comparisons are given. A dedicated FE-based program has been applied. The radiation patterns have been obtained by evaluating the vectorial Huygens principle.**

***Keywords*—Bluetooth, Finite elements, Vectorial Huygens principle, ground dependent antenna.**

I. Introduction

The recent increase of the use of wireless connections between computers and peripheral equipment enforces a deeper look into the radiation behavior of the appropriate antennas. For short distance communication Bluetooth has become a standard. It operates in the unlicensed, open frequency range between 2.4 and 2.485 GHz. With USB connected Bluetooth antennas, a wireless LAN may be established.

In general the external USB antennas are manufactured with double-sided printed circuit boards (PCB's). One side operates as ground whereas the other side contains a special characteristic antenna structure, eg. meander lines, F-forms, etc. Fig. 1 shows the structure of the standard antenna under investigation.

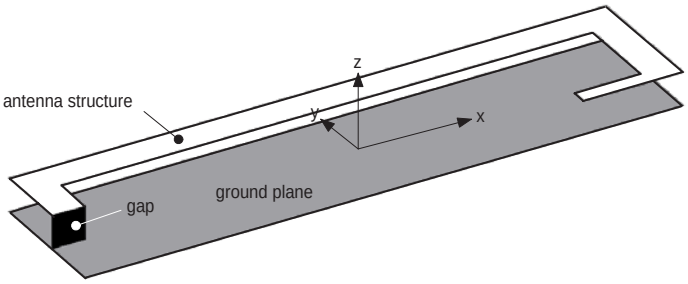

Fig. 1. Geometry of the Bluetooth antenna under investigation.

For use with notebooks, the Bluetooth antenna may be connected to a USB-plug. Illustrated in Fig. 2 is the typical arrangement. On the metallic side panel of the notebook case, the USB-antenna is connected and a short distance aside, a human forearm handles an external PC-mouse.

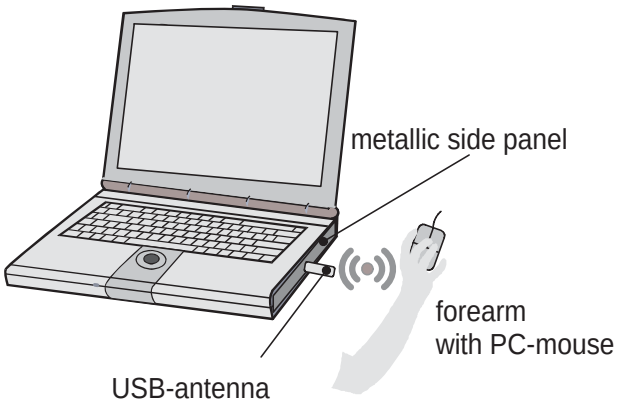

Fig. 2. USB-plugged antenna with environment.

The metallic side panel operates like an electric wall and reflects the electromagnetic wave. Two scenarios have been studied, thereby. The panel alone and a plastics coated side panel have been compared to each other.

The typical class - II radiator with a range up to 10 meters uses 2.5 mW of power, only. Hence, the power absorption in human tissue within the radiation range mentioned may be negligible. In contrast a great interference of the mouse handling forearm on the radiation characteristic is expected. For this case, the change in the radiation patterns will be documented, as well.

II. Numerical Model

The electromagnetic field problem has been solved with a FE-code based on the standard $\vec{A}v$ -formulation [1]. With the potentials $\vec{A}$ and v the field intensities for time harmonic variations follow:

$$\vec{E} = -j\omega\vec{A} - j\omega\nabla v, \tag{1}$$

$$\vec{H} = [\frac{1}{\mu}]\nabla \times \vec{A}. \tag{2}$$

The displacement current density is considered completely by treating the conductivity as a complex quantity $\underline{\sigma}_c$. Ampere's Law for the time harmonic case leads to

$$\nabla \times \vec{H} = \sigma\vec{E} + \epsilon\frac{\partial\vec{E}}{\partial t} = \underline{\sigma}_c\vec{E} \tag{3}$$

with

$$\underline{\sigma}_c\vec{E} = (\sigma + j\omega\epsilon)\vec{E}. \tag{4}$$

Manuscript received April 26, 2006

W. Renhart, K. Hollaus, C. Magele, G. Matzenauer and B. Weiss are with the Institute for Fundamentals and Theory in Electrical Engineering, Graz University of Technology, Kopernikusgasse 24, A-8010 Graz, Austria. e-mail: werner.renhart@tugraz.at

In $\underline{\sigma}_c$ the real part represents the physical electric conductivity σ. Therewith, the conducting current density is considered whereas the imaginary part of $\underline{\sigma}_c$ describes the displacement current density. Consequently, lossy, permittive media like human tissue at electromagnetic radiation can be treated as well.

The FE-mesh truncation has been realized by applying perfectly matched layers (PMLs), as recommended, eg. in [2].

In the FE-model, the antenna is modeled with the aid of boundary conditions. Along the grounded plane as well as along the antenna structure the electric scalar v and the tangential of $\vec{A}$ have been enforced to be zero. This allows the displacement current density to appear in normal direction to the antenna surface, only. Along the antenna gap the tangential of $\vec{A}$ has been prescribed and the electric scalar v has been set to zero. With this, from (1) follows:

$$\vec{E} \cdot \vec{e}_z \triangle z = -j\omega A_z \triangle z = -U_0. \tag{5}$$

$\vec{e}_z$ is therein the unit vector in z-direction (Fig. 1) and $\triangle z$ represents the gap width where the electric voltage U_0 is impressed. To compute the antenna radiation pattern for the various configurations, the vectorial Huygens principle [3] has been used.

For the sake of reliability the results have been compared to solutions obtained with a dedicated FDTD-package [4].

III. Numerical results

The simulations have been applied to a standard Bluetooth ground plane dependent antenna at a frequency of 2.4 GHz. Its gap width amounts to $\triangle z$=1 mm.

In order to show the variety of radiation patterns the directivity of the different configurations have been compared. As defined in [5] it expresses the ability of a radiator to focus the radiation in a particular direction. Considering spherical polar coordinates with the azimuthal angle Φ and the polar angle Θ it follows, depending on the components of the field intensity $\vec{E}$:

$$D_\phi(\phi,\Theta) = 2\pi \frac{|E_\phi(\phi,\Theta)|^2}{2\eta_0 P} \tag{6}$$

$$D_\Theta(\phi,\Theta) = 2\pi \frac{|E_\Theta(\phi,\Theta)|^2}{2\eta_0 P}. \tag{7}$$

η_0 is the characteristic impedance of free space and P presents the time-average power radiated per unit area, averaged over all directions in the far field.

A. General configuration

From the antenna environment shown in Fig. 2 not all parts in detail could be translated into the FE-model. Fig. 3 shows the objects modeled in principle.

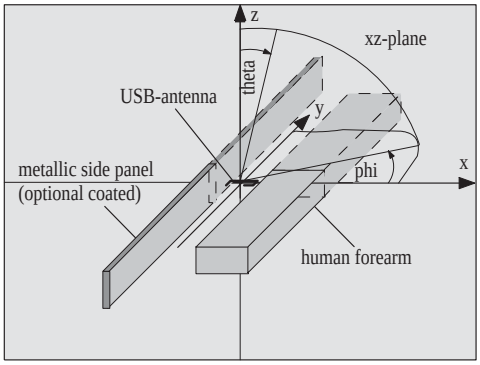

Fig. 3. Schematic drawing of the objects considered in the FE-model.

The metallic side panel length of 0.3 m has been measured from a standard notebook case. All other notebook case components have been disregarded. Definitely, a small influence to the radiation behavior is given. Its significance is assumed to be very small compared to the reflecting effect of the side panel. Additionally, the side panel can be coated by a synthetic material of $\epsilon_r = 4$ in the FE-model.

Midway positioned in the panel is the USB-plug with the antenna. Only 20 mm aside the antenna a PC-mouse operating forearm may be situated. This forearm has been modeled as a rectangular cuboid with homogenous material properties of $\sigma = 0.5S/m$ and $\epsilon_r = 10$. For the radiation pattern it is not important to model in detail the different layers of the forearm, like skin, muscles, fat and bone. Hence, mid-values have been chosen.

B. FEM and FDTD results in comparison

At first, the single antenna without any environmental objects has been computed with a FEM- and a FDTD-based code in order to gain reliability in the models developed.

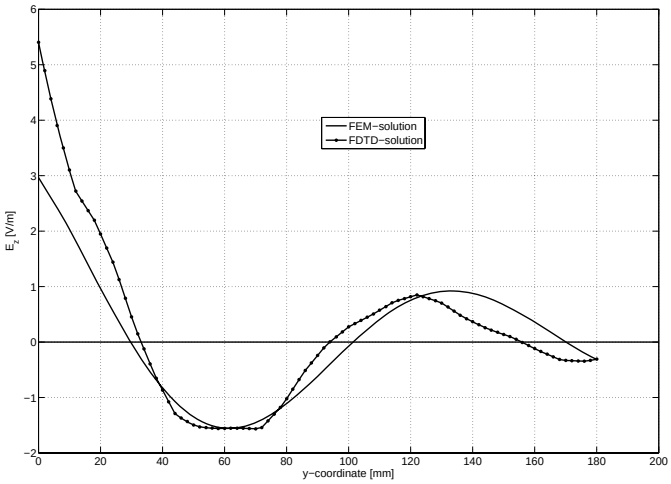

Fig. 4. FEM- and FDTD solution of E_z in comparison.

Especially, a correct choice of the PML-parameters must be ensured. So, along a line in y-direction off the antenna the z-component of the electric field intensity $\vec{E}$ has been compared. Fig. 4 shows the developing of the z-component of $\vec{E}$ up to the PMLs. Taking the modeling of first order absorbing boundary conditions [6] in the FDTD-procedure into account a sufficiently close solution of both computations can be observed. This points at an effectual attenuation of the incident wave within the PMLs in the FEM-model.

C. Antenna with metallic side panel

Subsequently, the USB-antenna with the metallic side panel has been computed. The comparison of this solution with the free space radiating solution is shown below. Therein, the point-marked curve represents the free space solution and the solid curve implies the solution with the side panel.

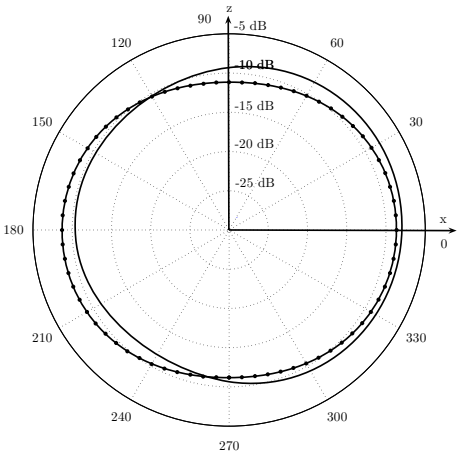

Fig. 5. Directivity, D_Φ in the xz-plane.

The diagram in Fig. 5 indicates a non-significant variation in the pattern of D_Φ. In case the side panel is present, the radiation characteristic diverges only slightly from the primary one.

A more rigorous change can be observed for D_Θ in Fig. 6. Nearly in all directions a significant decay in the radiation appears.

One should keep in mind, that the magnitude of the Φ-component of the E-field is about 10 dB smaller compared with the Θ-component.

D. Plastics coated metallic side panel

Next, the deviation of the radiation pattern for a plastics coated side panel has been investigated. For the computation the plastic coating has been modeled as a layer of 2.0 mm of thickness. To show the impact of the layer explicitely, the results have been compared with the non-coated side panel patterns.

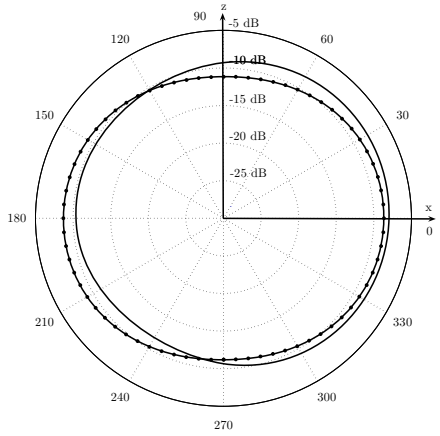

Fig. 6. Directivity, D_Θ in the xz-plane.

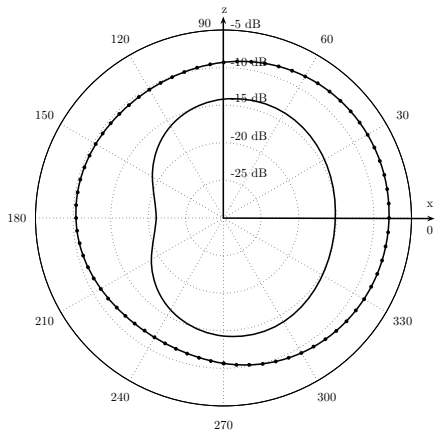

Fig. 7. Directivity D_Φ, plastics coated side panel.

The non-coated results correspond to the point-marked curves. As can bee seen in Fig. 7, a high deviation in the directivity of D_Φ is evident. The characteristic of the curves changes from a more ore less cirucular loop to a kidney like shape and the magnitude decreases up to -10 dB.

In opposite to the directivity D_Φ a non significant influence of the coating layer on the Θ-characteristics is found (Fig. 8).

E. Antenna with metallic side panel and human forearm

In the end the influence of a human forearm has been examined. In the FE-model the unfavorable case of the human tissue located very closely to the antenna has been

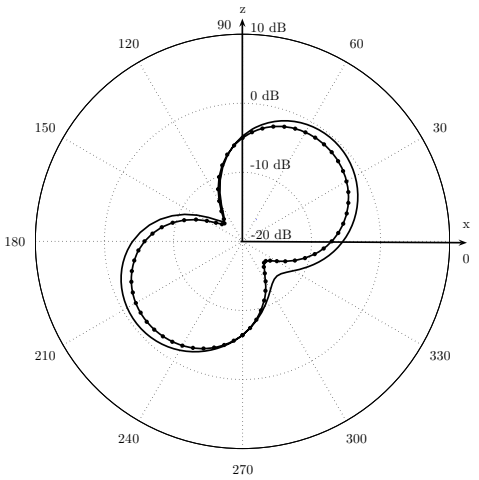

Fig. 8. Directivity D_Θ, plastics coated side panel.

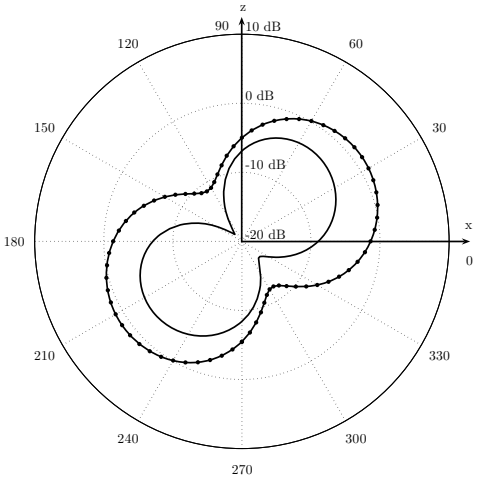

Fig. 10. Directivity D_Θ, side panel and human forearm.

considered. Again, the comparisons have been accomplished with the free space solutions, which correspond to the point-marked lines in the consecutive figures.

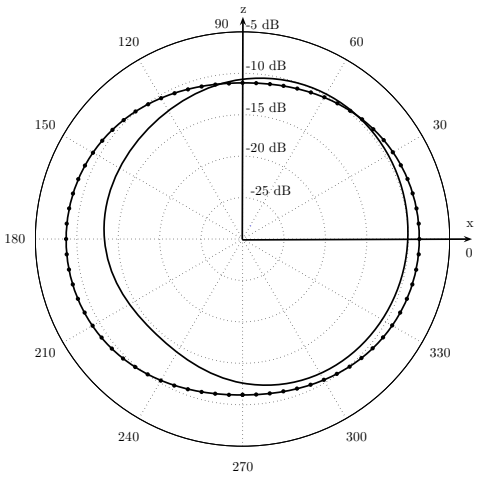

Fig. 9. Directivity D_Φ, side panel and human forearm.

Fig. 9 shows a major reduction of D_Φ to the left side whereas the radiation to the right half plane remains nearly unaffected.

Yet for the larger component of the E-field, its characteristics turns for the worse, as shown in Fig. 10. Into all directions the decrease of D_Θ becomes significant. This configuration reduces the requested operational reliability of a wireless LAN connection in Bluetooth-technology significantly.

IV. Conclusion

Several configurations to investigate the influence of environmental objects to the radiation pattern of a USB-connected Bluetooth antenna have been computed. For the standard antenna in use, it turned out that the directivity D_Φ for all cases is of minor magnitude than the Θ-component. However, the change in the patterns for D_Φ obviously is higher. Concerning D_Θ for all cases examined the characteristics remain like a bended eight. But its magnitude varies strongly. It turned out that the worst configuration is given when the human forearm operates in the vicinity of the antenna peak. For this case only, a reliable wireless LAN connection via Bluetooth over middle distances may not be given.

References

[1] O. Biro, "Edge element formulations of eddy current problems", *Computer methods in applied mechanics and engineering*, vol. 169, pp. 391-405, 1999.

[2] I. Bardi et. al., "Parameter Estimation for PML's Used with 3D Finite Element Codes", *IEEE Trans. Magn.*, Mag-34, pp. 2755-2758, 1998.

[3] K. Simonyi, "Theoretische Elektrotechnik", *Barth-Verlag, Leipzig*, 10. Aufl., 1993, p. 880 ff.

[4] K. Hollaus et al., "Simulation of Simple Topologies on a PCB by a Frequency and a Time Domain Method", *Proceedings of Joint 9th ICEAA '05 and 11th EESC '05*, ISBN 88-8202-094-0, pp. 893-896.

[5] G.S. Smith, "An introduction to classical electromagnetic radiation", *Cambridge University Press*, ISBN 0 521 58093, 5th ed., 1997, p. 218 ff.

[6] G. Mur, "Absorbing Boundary Conditions for the Finite-Difference Approximation of the Time-Domain Electromagnetic-Field Equations", *IEEE Trans. Electromagn. Compat.*, vol. 23, pp. 377-382, Nov. 1982.